ACTA ONCOLOGICA
2022, VOL. 61, NO. 2, 264–268
https://doi.org/10.1080/0284186X.2021.2022203

Taylor & Francis
Taylor & Francis Group

LETTER TO THE EDITOR

Impact of curing conditions on basic dosimetric properties of silicone-based radiochromic dosimeters for photon and proton irradiation

Morten B. Jensen[a,b,c], Lia B. Valdetaro[a,b*], Peter Balling[d,e], Peter S. Skyt[a], Jørgen B. B. Petersen[c], Simon J. Doran[f], Mateusz K. Sitarz[a] and Ludvig P. Muren[a,b]

[a]Danish Centre for Particle Therapy, Aarhus University Hospital, Aarhus, Denmark; [b]Department of Clinical Medicine, Aarhus University, Aarhus, Denmark; [c]Department of Medical Physics, Aarhus University Hospital, Aarhus, Denmark; [d]Department of Physics and Astronomy, Aarhus University, Aarhus, Denmark; [e]Interdisciplinary Nanoscience Center, Aarhus University, Aarhus, Denmark; [f]The Institute of Cancer Research, London, UK

ARTICLE HISTORY Received 27 June 2021; Accepted 18 October 2021

Introduction

Advances in radiotherapy (RT) have, over the years, led to an increase in the complexity of treatment delivery techniques. Intensity-modulated RT, volumetric-modulated arc therapy, and proton therapy (PT) can deliver highly conformal dose distributions with steep dose gradients, demanding dose verification in three dimensions (3D) with a high spatial resolution [1,2]. Polymer gels, radiochromic gels, and radiochromic plastics can record radiation dose distributions in 3D, supplementing ionization chambers and planar dosimeters, such as films [3,4].

A deformable silicone-based radiochromic 3D dosimeter composed of a radiosensitive dye, leucomalachite green (LMG), dispersed in a silicone matrix was first proposed in 2015 [5,6]. Key dosimetric properties have been extensively characterized, demonstrating the clinical potential for conventional RT [5–9] and magnetic resonance imaging-guided RT (MRgRT) [10], as well as for passive and spot-scanning proton therapy [11,12].

Radiochromic dosimeters register dose if a chemical reaction chain takes place: radiation interacts with the initiator, creating oxidizing reagents which can oxidize the LMG molecules, producing malachite green (MG), a blue/green colored molecule, changing the wavelength-dependent optical attenuation coefficient of the material [2,3]. However, if a competing chemical reaction occurs, e.g., radical recombination, or other secondary processes, the reactants will not interact with LMG molecules, and the 'registered' dose will be lower than the dose deposited to the dosimeter [11]. Higher dose rates likely lead to an increase in competing reactions and, consequently, signal quenching [11,12]. Linear-energy-transfer (LET) signal quenching is also present in radiochromic dosimeters [11]. However, this study focused on the low-LET regime, so dose-rate could be investigated separately.

Typical proton beam scanning (PBS) treatment delivery has a much higher dose-rate range than what can be obtained with conventional LINACs [11,12], presenting bigger challenges when it comes to dose-rate independence. There would still be a major advantage in decreasing dose-rate dependency for protons in the typical range for clinical plans since a quenching correction model parametrizing dose-rate dependency can be complex and time-consuming [12].

Previous studies have identified a formulation that shows insignificant dose-rate dependency for photon irradiation in both conventional RT and MRgRT [9,10,13]. However, the dosimetric properties of radiochromic dosimeters can vary significantly for different curing procedures [14–17] and must be investigated.

The aim of this study was therefore to assess different dosimeter compositions and curing times to optimize the balance between dose-rate dependency and dose response for photon and proton irradiation in clinically relevant beams.

Material and methods

Fabrication and curing conditions

Dosimeters were fabricated from silicone elastomer (SE), curing agent (CA), LMG, and chloroform following a previously established protocol [5,8]. The SE and CA come from the commercially available SYLGARD 184 elastomer (DOW, Corning) kit. Two different chemical compositions were used, containing (in total weight percentage) either 0.26% LMG, 1.5% chloroform, 5% CA and 93.2% SE or 0.26% LMG, 1.5% chloroform, 9% CA, and 89.2% SE. LMG was dissolved in chloroform and then mixed with SE and CA using a mixer before air bubbles were removed using a vacuum desiccator, poured into optical polystyrene cuvettes (1 × 1 × 4.5 cm, with a wall thickness of 1 mm), and left to cure protected from light. The dosimeters were made from 5 batches;

CONTACT Morten B. Jensen mobjje@rm.dk Danish Centre for Particle Therapy, Aarhus University Hospital, Aarhus, Denmark
*Equally contributing first author.

Supplemental data for this article can be accessed here.

Batches 1 and 4 had 5% CA, while the remaining had 9% CA. Batch 3 was cured at 15 °C while the other batches were cured at 20 °C (see Supplementary Table S1).

Photon irradiation

Dosimeters were irradiated with photons using a Varian TrueBeam linear accelerator at Aarhus University Hospital, with a 6 MV beam quality and fixed machine-set dose rate. To obtain different irradiation conditions, the cuvettes were placed between a 5 cm solid water (SW) backscatter slab and 4.5, 9.5, and 14.5 cm SW build-up slabs, respectively, and irradiated to dose levels ranging from 5 to 20 Gy with a constant source-to-surface distance (SSD) of 95 cm, i.e., the treatment couch was corrected when adding additional SW build-up slabs. The different build-up slabs corresponded to dose rates ranging from 3.3 to 6.0 Gy/min. See Supplementary Material for a detailed description and experimental setup.

Proton irradiation

Irradiation with protons was performed with a Varian ProBeam isochronous cyclotron at the Danish Centre for Particle Therapy at Aarhus University Hospital, with a spot-scanning monoenergetic beam of 100 MeV, delivering an 8 × 4 cm uniform field. Five cuvettes were placed perpendicularly to the beam direction between 1 cm build-up and 30 cm backscatter SW slabs and irradiated to dose levels of 5, 10, and 15 Gy. The field had very low linear-energy-transfer (LET) in the region investigated, with dose-averaged LET of ~0.85 keV/μm in water (calculated with Libamtrack) [18]. Dose rates were 23, 74, and 95 Gy/min (defined at 2 cm depth in water). The lowest dose rate (23 Gy/min) was associated with the lowest stable beam current at the nozzle. For a detailed description see Supplementary Material.

Read-out and definition of dose response

Dosimeters were read out 2 h before and 2 h after irradiation. The cuvettes were read out at 635 nm using a spectrophotometer (Spectroquant Pharo 100). The dose response was given by the slope when plotting the difference in attenuation coefficient measured after and before irradiation against dose. We investigated dose-rate dependency by analyzing the variation between dose response as a function of dose rate for each batch and curing time.

Results

For photons, the greatest variation between dose responses as a function of dose rate were 3, 4, and 4% for 1, 3, and 5 days of curing for Batch 1 (5% CA—curing temperature 20 °C) and 7, 4, and 1% for Batch 2 (9% CA—curing temperature 20 °C), respectively. For the batch curing at 15 °C for 2 days, the greatest variation was found to be 6%. The dose response decreased with curing time. For Batch 1 the dose response for 3 and 5 days of curing decreased to 79 and 77% and for Batch 2 it decreased to 69 and 57% when compared to 1 day of curing for a dose rate of 3.3 Gy/min. The 9% CA curing for 1 day at 20 °C and 2 days at 15 °C had non-overlapping confidence intervals for the three dose rates (Figures 1 and 2, Supplementary Table S2).

For protons, we did not observe a decrease in dose-rate dependency for any composition curing for 1, 3, and 5 days at 20 °C when comparing the lowest dose rate (23 Gy/min) to 74 and 95 Gy/min, with a difference in dose response ranging from 21 to 30%. There was no significant difference between dose responses for cuvettes irradiated with dose rates of 74 and 95 Gy/min, with overlapping confidence intervals for the two dose rates except for 5% CA curing for 5 days (Figures 1 and 2, Supplementary Table S3).

Discussion

This study investigated the dose-response and dose-rate dependencies for different compositions and curing conditions for silicone-based radiochromic dosimeters. For the 5% CA photon irradiation, we found no significant change in dose-rate dependency and a decrease in dose response for longer curing time. Whereas for the 9% CA photon irradiation, there was a decrease in dose-rate dependency and dose response with curing time. For protons, we found no dose-rate dependency between the two higher dose rates investigated (74–95 Gy/min) for both CA compositions except for 5% CA curing for 5 days.

In the radiochromic dosimeter, chloroform is believed to be the main initiator or source of radical production. That is an integral part of the chain process that leads to a measurable signal, i.e., conversion of LMG into MG [4,11]. However, molecules that are not chemically cross-linked but originate from the silicone elastomer can be another source of free radicals—explaining the higher dose response for the 5% CA group when compared to the 9% CA. The incomplete cross-linking of silicone elastomer can be due to a lower ratio of curing agent than specified by the manufacturer (1:10), and/or the dosimeters not having cured completely (they are still malleable). We can understand the mechanism behind dose-rate dependency by turning to track structure theory [19,20]. In this theory, dosimeters are described as discrete radiosensitive elements dispersed in a matrix, which can be activated by one or several 'hits' (an interaction that leads to a measurable signal) from ionization radiation. However, if a concurrent process occurs, e.g., radical recombination, secondary reactions, etc., radiosensitive elements are not 'hit' and, thus, the signal is lost. Since higher dose-rate beams have a larger radical production rate, there are more radicals to recombine with increasing the probability that a process that does not generate a 'hit' will occur, which leads to lower dose response for higher dose rates. Thus, by lowering the concentration of free radicals for longer curing times, the dependency was expected to decrease. Additionally, the similar dose response observed for very high proton dose rates could indicate that the rate of incident ionizing radiation exceeded the characteristic recombination/secondary reactions time scale. LET dependency for protons can be

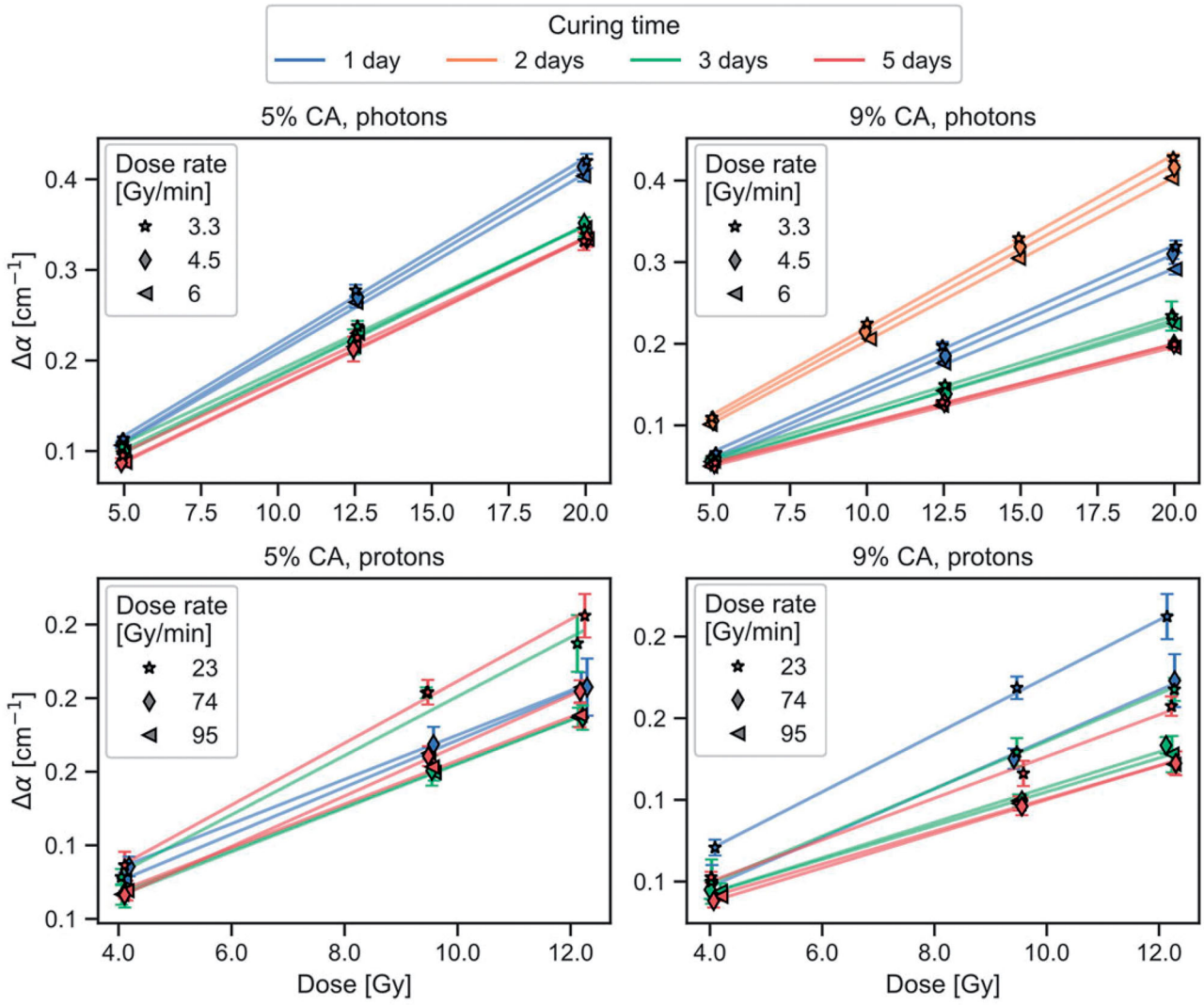

Figure 1. Top: Optical response as a function of dose for photon irradiation (five cuvettes per dose point). Error bars represent 95% confidence intervals, with $R^2 > 0.99$ for all regression models. The 9% CA curing for 2 days had dose rates of 3.5, 4.6, and 6.0 Gy/min. Bottom: Optical response as a function of dose for proton irradiation (five cuvettes per dose point), with $R^2 > 0.97$ for all regression models. Different irradiation days are indicated by color, and markers indicate dose rate. A small offset was applied on the x-component (dose), since the overlap made it hard to distinguish individual data points.

explained with similar track-structure arguments. However, the proton energy in this study corresponded to a dose-averaged LET < 1 keV/μm, so there was a very small LET dependency (see Supplementary Section 5).

In previous studies concerning dose-rate dependency, the dose rate was changed by varying the machine-set dose rate, i.e., the time between pulses delivered by the linear accelerator while keeping the instantaneous fluence constant [9,11,13]. In this study, the photon dose rate was changed by adding additional SW build-up slabs with constant SSD, thus changing the instantaneous fluence, while keeping constant the time between pulses [10].

This study focused mainly on dose-response and dose-rate dependencies. However, temporal stability (i.e., how the dose response evolves as a function of read-out time after irradiation), background-color (i.e., the optical density at the time of read-out before irradiation) and the stiffness of the dosimeter should also be considered when deciding on a protocol for fabrication. The dose response has been shown to decrease as the time from irradiation to read-out increases [5,17]. Du et al. [17] investigated self-coloring of irradiated and non-irradiated 9% CA dosimeters—a phenomenon they term 'creep-up effect'. Creep-up effects reduce the accuracy of 3D optical-CT read-out for phantoms with high values of optical density [21]. Therefore, compositions with as low background color as possible are preferred. The optical density of the background color was lower for the 9% CA compared to the 5% CA when cured for 3 and 5 days (Supplementary Figure S2).

The dose responses found in this study were comparable to previous investigations [9–11,17]. Differences are attributed to batch-to-batch dependence, time in between read-outs and irradiation, read-out wavelength, curing time, curing temperature, and light-exposure history.

The Young's modulus of the dosimeter, which gives a measure of how easily the material can be bended or stretched, increases with curing time and with the amount of CA [22]. Consequently, for deformation studies, the 5% CA

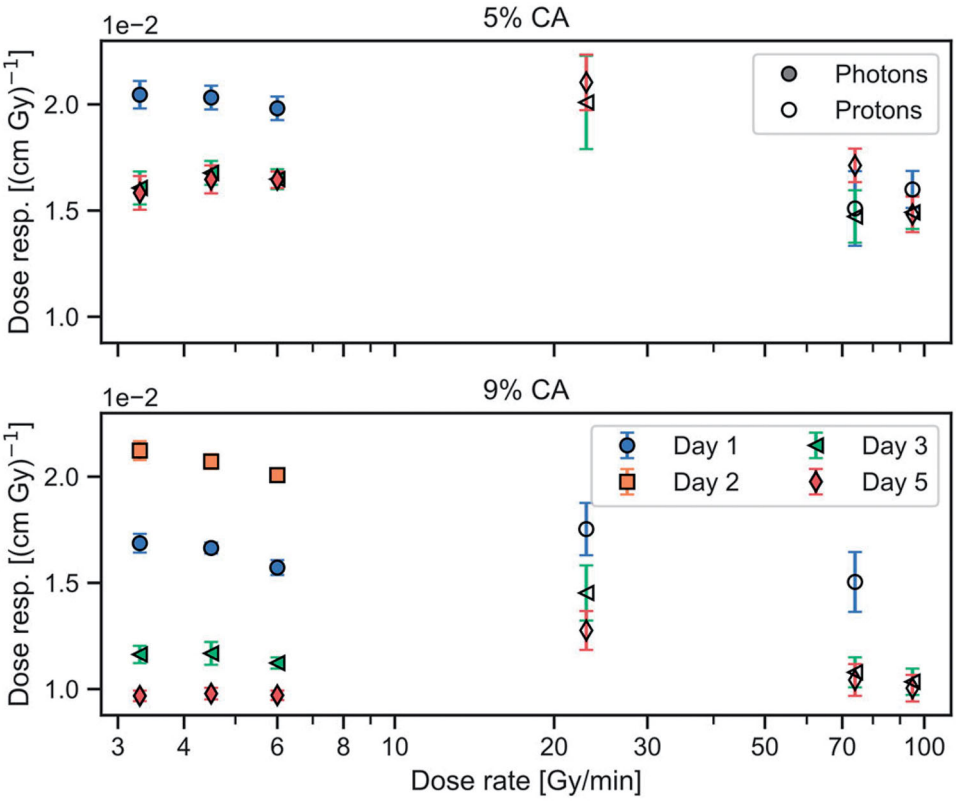

Figure 2. Dose response as a function of dose rate for photon (filled markers) and proton (hollow markers) irradiation. Error bars represent 95% confidence intervals in each group. The 2-day curing 9% CA had a curing temperature of 15 °C on the contrary to the other dosimeters curing at 20 °C (see Supplementary Material for specific batches).

composition is favored over the 9% CA. The mechanical properties are of particular interest since these dosimeters are unaffected when irradiated with protons during various stages of deformation [23].

In conclusion, we found that longer curing times reduced the dose-rate dependency but led to a decrease in dose response. Batches containing 5% CA had a higher dose response compared to the 9% CA. Lowering the curing temperature increased the dose response (only investigated for one chemical composition). The composition containing 9% CA has favored over 5% CA in terms of background color, but it is stiffer, hindering deformation experiments. Therefore, the choice of composition depends on what prospective studies want to investigate. This study indicated that three days of curing presents an optimal balance between dose-rate dependency, dose response, and background color for both compositions. Future work will characterize larger samples, to access if the dosimetric properties found in this study can be translated directly.

Disclosure statement

No potential conflict of interest was reported by the author(s).

Funding

This research is funded by the Novo Nordisk Foundation (Grant number NNF18OC0034718).

ORCID

Morten B. Jensen http://orcid.org/0000-0003-3343-8837
Lia B. Valdetaro http://orcid.org/0000-0002-2810-4878
Peter Balling http://orcid.org/0000-0003-4955-770X
Peter S. Skyt http://orcid.org/0000-0002-9710-6711
Jørgen B. B. Petersen http://orcid.org/0000-0001-9225-876X
Simon J. Doran http://orcid.org/0000-0001-8569-9188
Ludvig P. Muren http://orcid.org/0000-0002-7418-5832

References

[1] Wuu CS, Xu Y. Three-dimensional dose verification for intensity modulated radiation therapy using optical CT based polymer gel dosimetry. Med Phys. 2006;33(5):1412–1419.
[2] Oldham M, Sakhalkar H, Guo P, et al. An investigation of the accuracy of an IMRT dose distribution using two- and three-dimensional dosimetry techniques. Med Phys. 2008;35(5):2072–2080.
[3] Baldock C, De Deene Y, Doran S, et al. Polymer gel dosimetry. Phys Med Biol. 2010;55(5):R1–R63.
[4] Oldham M. Radiochromic 3D detectors. J Phys Conf Ser. 2015;573:012006.
[5] Høye EM, Skyt PS, Yates ES, et al. A new dosimeter formulation for deformable 3D dose verification. J Phys Conf Ser. 2015;573:012067.
[6] De Deene Y, Hill R, Skyt PS, et al. Flexydos3D: a new deformable anthropomorphic 3D dosimeter readout with optical CT scanning. J Phys Conf Ser. 2015;573:012025.
[7] De Deene Y, Skyt PS, Hil R, et al. FlexyDos3D: a deformable anthropomorphic 3D radiation dosimeter: radiation properties. Phys Med Biol. 2015;60(4):1543–1563.
[8] Høye EM, Sadel M, Kaplan L, et al. First 3D measurements of proton beams in a deformable silicone-based dosimeter. J Phys Conf Ser. 2017;847:12021.

[9] Høye EM, Balling P, Yates ES, et al. Eliminating the dose-rate effect in a radiochromic silicone-based 3D dosimeter. Phys Med Biol. 2015;60(14):5557–5570.
[10] Jensen MB, Balling P, Doran SJ, et al. Dose response of three-dimensional silicone-based radiochromic dosimeters for photon irradiation in the presence of a magnetic field. Phys Imaging Radiat Oncol. 2020;16:81–84.
[11] Hoye EM, Skyt PS, Balling P, et al. Chemically tuned linear energy transfer dependent quenching in a deformable, radiochromic 3D dosimeter. Phys Med Biol. 2017;62(4):N73–N89.
[12] Valdetaro LB, Høye EM, Skyt PS, et al. Empirical quenching correction in radiochromic silicone-based three-dimensional dosimetry of spot-scanning proton therapy. Phys Imaging Radiat Oncol. 2021;18:11–18.
[13] Carpentier EE, Alexander KM, Todd S, et al. Characterization of a radiochromic silicone dosimeter. J Phys Conf Ser. 2017;847:012052.
[14] Wheatley MJ, Booth JT, De Deene Y. Evaporation and diffusion of chloroform with the deformable FlexyDos3D radiation dosimeter. J Phys Conf Ser. 2019;1305(1):012044.
[15] Wheatley MJ, Balatinac AS, Booth JT, et al. Physico-chemical properties and optimization of the deformable FlexyDos3D radiation dosimeter. Phys Med Biol. 2018;63(21):215028.
[16] Wheatley MJ, Balatinac AS, Booth JT, et al. Optimization for stability of the deformable FlexyDos3D radiation dosimeter and curing effects. J Phys Conf Ser. 2019;1305(1):012030.
[17] Du Y, Wang R, Yue H, et al. Dose response and stability of silicone-based deformable radiochromic dosimeters (FlexyDos3D) using spectrophotometer and flatbed scanner. Radiat Phys Chem. 2020;168:108574.
[18] Greilich S, Grzanka L, Bassler N, et al. Amorphous track models: a numerical comparison study. Radiat Meas. 2010;45(10):1406–1409.
[19] Butts JJ, Katz R. Theory of RBE for heavy ion bombardment of dry enzymes and viruses. Radiat Res. 1967;30(4):855–871.
[20] Pedro A, Burns DT, Nahum AE, et al. Chapter 13, chemical dosimeters. In: Fundamentals of ionizing radiation dosimetry. Weinheim: Wiley; 2017. p. 568–574.
[21] Al-Nowais S, Doran SJ. CCD-based optical CT scanning of highly attenuating phantoms. J Phys Conf Ser. 2009;164:012023.
[22] Kaplan LP, Høye EM, Balling P, et al. Determining the mechanical properties of a radiochromic silicone-based 3D dosimeter. Phys Med Biol. 2017;62(14):5612–5622.
[23] Jensen SV, Valdetaro LB, Poulsen PR, et al. Dose-response of deformable radiochromic dosimeters for spot scanning proton therapy. Phys Imaging Radiat Oncol. 2020;16:134–137.